Ultrasensitive nonlinear vibrational spectroscopy of complex molecular systems

Selig, O.

Publication date
2017
Document Version
Other version
License
Other

Chapter 7

Real-Time Observation of Organic Cation Reorientation in Methylammonium Lead Iodide Perovskites[a]

The introduction of a mobile and polarised organic moiety as a cation in three-dimensional lead-iodide perovskites brings fascinating optoelectronic properties to these materials. The extent and the timescales of the orientational mobility of the organic cation and the molecular mechanism behind its motion remain unclear, with different experimental and computational approaches providing very different qualitative and quantitative description of the molecular dynamics. Here we use ultrafast two-dimensional vibrational spectroscopy of methylammonium (MA) lead iodide, to directly resolve the rotation of the organic cations within the $MAPbI_3$ lattice. Our results reveal two characteristic time constants of motion. Using ab-initio molecular dynamics simulations, we identify these as a fast (∼300 fs) 'wobbling-in-a-cone' motion around the crystal axis, and a relatively slow (∼3 ps) jump-like reorientation of the molecular dipole with respect to the iodide lattice.

[a] Adapted from: A. A. Bakulin, O. Selig, H. J. Bakker, Y. L. A. Rezus, C. Müller, T. Glaser, R. Lovrincic, Z. Sun, Z. Chen, A. Walsh, J. M. Frost, T. L. C. Jansen, "J. Phys. Chem. Lett.", **6**, 3663-3669 (2015)

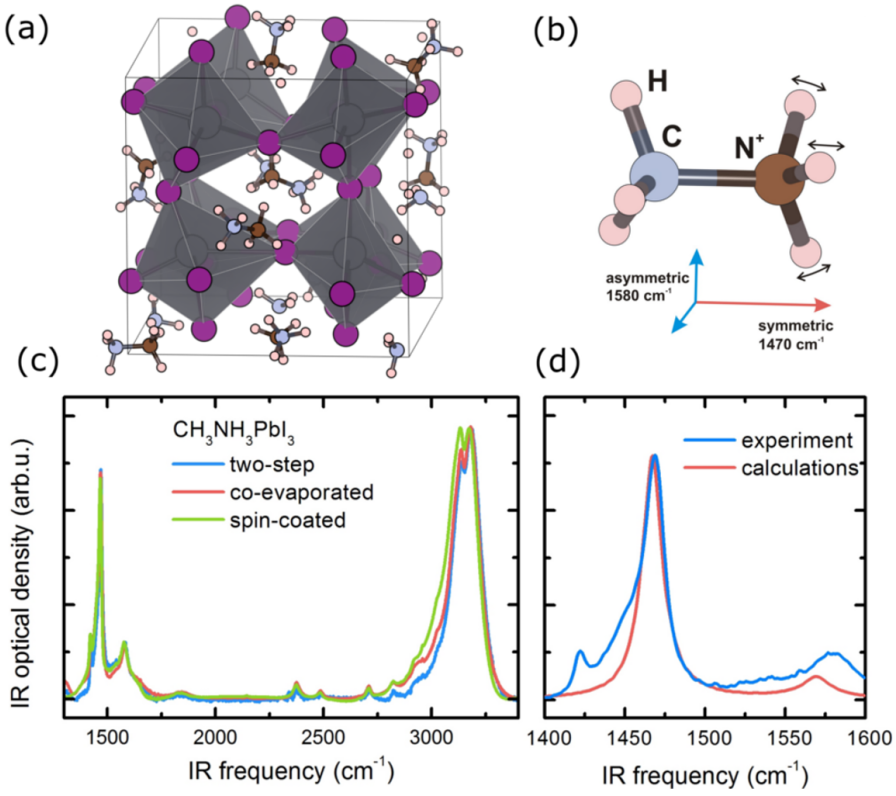

FIGURE 7.1. Perovskite material under study: (a) A snapshot from a molecular dynamics simulation showing the structure of the $MAPbI_3$ perovskite. (b) The MA molecule and the orientation of the transition dipoles of the NH_3^+ bending vibrations. (c) IR absorption spectra of $MAPbI_3$ films prepared using different methods. (d) Absorption spectra of a $MAPbI_3$ film in the NH/CH bending vibrational region. The red line shows the calculated absorption spectrum of the NH_3 bending modes (on the basis of the MD simulation).

7.1 INTRODUCTION

Hybrid organic-inorganic perovskites[191] are attracting a lot of attention for optoelectronic applications as they combine the solution processability of molecular electronic materials with the low exciton binding energy and high charge mobility of inorganic sesmiconducting crystals.[192,193] Many of these features can be related to the high dielectric constant of the material. The recent breakthroughs achieved by the application of methylammonium ($CH_3NH_3^+$ or MA) lead halides[194] in photovoltaic[195–197] and light-emitting[198] devices have triggered extensive research efforts to unravel the fundamental photophysics of these material systems. The organic cations, like MA, are not directly involved in the makeup of the valence or conduction bands. Yet they are shown to have a strong influence on the

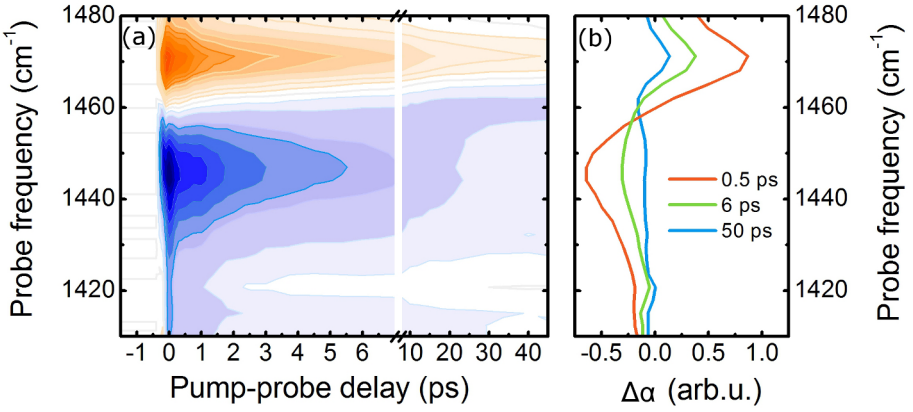

FIGURE 7.2. (a) Isotropic pump-probe transient spectra of a co-evaporated perovskite film measured using broadband excitation. (b) Isotropic pump-probe responses at different pump-probe delay times.

optoelectronic properties of the perovskites.[199,200] The size and shape of the molecular cations, as well as their embedding in the lattice, determine the macroscopic and molecular-scale perovskite crystal structure,[199,201,202] which in turn determines the band gap[200,202] of the material via the deformation potential. This offers the opportunity to tune the material properties through modification of the organic cation.[200] Furthermore, some of the unique properties of hybrid perovskites may be associated with the asymmetry and preferential alignment or to the dynamics of the embedded molecules. In contrast to spherically symmetric inorganic (atomic) cations, organic ions have a less symmetric shape and can possess a permanent dipole moment.[200,203] As a result, the positioning, orientation and rotational dynamics[204] of the organic moiety within the inorganic lattice can have a strong influence on the electronic system.[205] The reorientation of the organic cation with its associated dipole moment contributes to the dielectric response, and applies a crystal field to the material; both will affect the photovoltaic action. However, recent results suggest that though the choice of organic moieties is critical for material performance,[206,207] cations do not dominate solar cell hysteresis[208] and are not essential in obtaining high open circuit voltages.[209] A number of optoelectronic phenomena associated with molecular cation motion have been proposed based on electronic structure calculations. Cations were proposed to be responsible for the variations in dielectric constants, para- and ferroelectric behaviour,[203,210,211] current-voltage hysteresis,[199,212–214] a decrease in exciton binding energy, charge carrier segregation in the material, and dynamic disorder in valence and conduction band energies.[215,216] Most of these effects are expected to be extremely sensitive to the interplay between cation-cation and cation-anion interactions, the orientational mobility of organic molecules and the time scales of the structural dynamics. The rotational mobility of organic cations in inorganic lattices has been studied for application-relevant lead-iodide and lead-bromide perovskites using MA as

the organic cation (Figure 7.1(a)). The first estimates for MA reorientation were obtained using NMR spectroscopy, which pointed towards 0.2–0.4 ps rotational correlation functions for the C–N and N(C)–H axes,[217] comparable to the time scale of the reorientation of similarly sized molecules in free space. Dielectric relaxation and calorimetry measurements confirmed the fast rotation and orientation disorder of MA in perovskite materials at room temperature.[218,219] However, some recent theoretical[220–222] and experimental[210,213,223–225] results present arguments towards much longer reorientation timescales of 5–14 ps. Clearly, at present there is insufficient understanding of hybrid perovskite structural dynamics. This understanding requires comprehensive and direct experimental-theoretical approach that would allow one to identify the mechanistic picture behind the different timescales of the atomic and molecular motions. In this chapter, we report on an ultrafast polarization-resolved two-dimensional infrared (2DIR) vibrational spectroscopy and ab-initio molecular dynamics (MD) study of the MA cation rotation for a set of $MAPbI_3$ materials. Using the NH_3^+ symmetric bending vibration as a probe, we observe two characteristic timescales of molecular motion, which we identify as a fast ($\sim$0.3 ps) wobbling-in-a-cone around the preferential MA dipole directions parallel to the lattice axes, and relatively slow (>2 ps) jump-like reorientation of the molecular dipole (aligned with the CN axis) with respect to the crystal lattice. This result suggests that in $MAPbI_3$ at room temperature the alignment of cation dipoles, if present, is likely to be of intermediate-range order.

7.2 RESULTS AND DISCUSSION

7.2.1 INFRARED SPECTROSCOPY

To tackle the potential effect of crystal defects and grain boundaries on cation dynamics, we investigated $MAPbI_3$ films made with three different techniques:

- multilayer spin-coating,
- a solvent-free two-step formation from PbI_2 and methylammonium-iodide (MAI) precursors,[226] and
- co-evaporation from $PbCl_2$ and MAI.[227,228]

The samples were prepared and characterized by the groups of Robert Lovrincic and Zhuoying Chen (for details see Ref.[229]). All films were deposited onto infrared (IR) transparent CaF2 substrates and had a thickness of $\sim$1 μm. To observe the dynamics of molecular reorientation we used ultrafast vibrational spectroscopy, with the symmetric NH_3^+ bending vibration as a probe. Figures 7.1(b)-(d) show the structure of the MA molecule and its contribution to the perovskite IR absorption spectrum in the vibrational fingerprint region.[230] The spectrum is dominated by the NH_3^+ stretching and bending modes in the regions of $\sim$3200 cm^{-1} and $\sim$1500 cm^{-1}, respectively. We attribute the weak narrow peaks in the regions around 2800 cm^{-1} and 1420 cm^{-1} to CH_3 stretching and bending vibrations. These peaks are much less pronounced than the NH_3^+ vibrations due to the relatively small transition

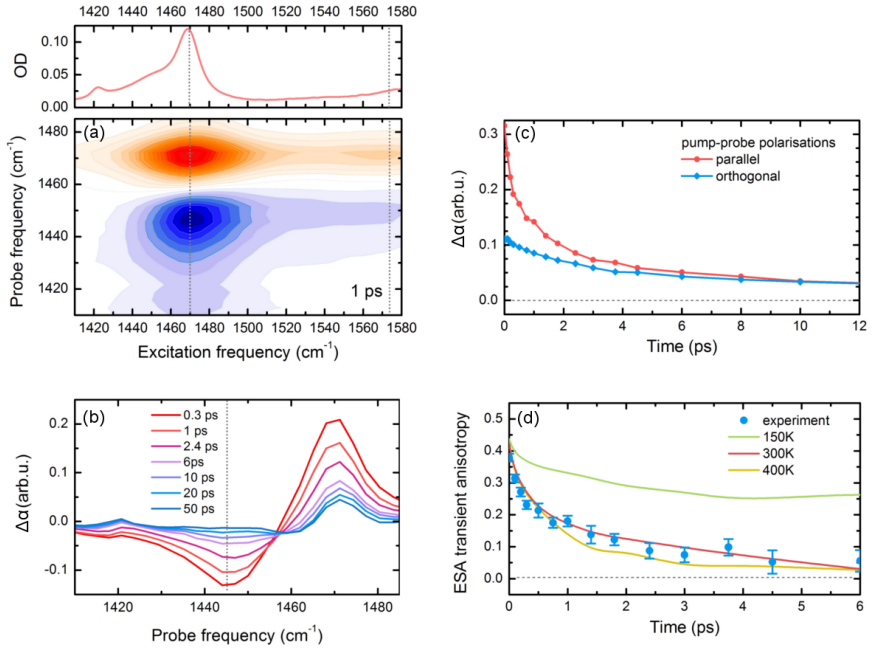

FIGURE 7.3. 2DIR response of NH bending vibrations: (a) Isotropic 2D spectra of co-evaporated perovskite film (average over three samples) 1 ps delay time. The different colours correspond to 5% steps from the maximum amplitude. Upper panel shows the corresponding absorption spectrum. (b) Cross sections through the 2D spectrum of the co-evaporated perovskite at ν_{ex}=1470 cm^{-1} for different delay times. (c) The dynamics of the excited-state absorption in the (ν_{ex} = 1470 cm^{-1}; ν_{pr} = 1445 cm^{-1}) point of 2D spectrum measured for parallel and orthogonal pump and probe pulses polarisations. (d) Anisotropy dynamics associated with the data in panel (c) with 95% confidence interval indicated. The solid lines represent the transient anisotropy dynamics calculated based on the MD simulations at different temperatures.

dipole moments of the CH vibrations as compared to the NH vibrations, and will not be adressed in this study. Due to the degeneracy of the three NH oscillators, both stretching and bending vibrations split into one symmetric and two asymmetric normal modes with orthogonal transition dipole moments. The symmetric bending mode at 1470 cm^{-1} is well separated in frequency from the asymmetric bending modes (Figure 7.1(d)) at 1580 cm^{-1} and has its transition dipole moment aligned along the C–N axis of the molecule. This makes it possible to use the transition dipole moment of the symmetric NH_3^+ bending vibration as a probe for the reorientation of the C–N bond and, thus, of the static dipole of the MA cation.

To measure the orientational dynamics of the symmetric NH_3^+ bending oscillator we performed polarization-resolved pump-probe and 2DIR experiments[77,231–233] on perovskite films in the 1400–1600 cm^{-1} frequency range (see Chapter 3 for experimental details). Using a collinear fast-scanning Mach-Zehnder scheme,[78]

molecular vibrations were first excited by an interferometric pair of strong 100 fs IR pump pulses. After a variable delay time, the excited state population was probed by weak broadband probe pulses with the polarizations parallel and orthogonal to the pump pulse. The isotropic signal and the anisotropy of the response were calculated as according to Eq 2.74 and Eq. 2.75, respectively. For non-interacting transition dipoles in an isotropic medium, the anisotropy decays from its initial value of 0.4 to 0, when the orientations of the transition dipoles are completely scrambled as a result of orientation diffusion. In the isotropic signal, the effect of the reorientation is completely removed, thereby only representing population relaxation. By scanning the delay between the two pulses of the interferometric pump we obtain a frequency resolution of $\sim$5 cm^{-1}.

We first present the pump-probe spectra for a co-evaporated $MAPbI_3$ film (Figure 7.2(a), (b)). In this measurement, only the isotropic component was extracted. At positive delay times, the bleaching/stimulated emission of the 0$\rightarrow$1 $NH_3{}^+$ symmetric bending transition is clearly observed at 1470 cm^{-1}. The excited state 1$\rightarrow$2 absorption from the first to the second excited state of the vibrational oscillator is observed at 1445 cm^{-1} and is anharmonically shifted from the 0$\rightarrow$1 transition by $\sim$25 cm^{-1}. The excited-state population decays on an timescale of 3 ps which should provide an observation window of up to 6 ps for the orientational dynamics. However, at long times we observe additional signals at 1475 cm^{-1} and 1420 cm^{-1}, which do not change significantly with time. These features coincide with the linear absorption peaks (Figure 7.1) and live for the times longer than 50 ps, which make us to assign them to a thermal response.[234] The relaxation of high-frequency bending vibrations creates multiple low-frequency excitations (a so-called hot ground state), which lead to the change in the absorption of the bending modes. The spectral overlap of the bleaching 0$\rightarrow$1 transition and the thermal response complicates the anisotropy analysis in this frequency range. Therefore, for later anisotropy analysis, we will only consider the data from the ESA probe region 1445 cm^{-1}, where the thermal signal is much smaller than population signal in the time window $<$10 ps, as can be seen from the spectra at long delay times. With this in mind, we will use the 2D-IR spectra to (i) decouple the 'clean' rotation-related anisotropy dynamics from the thermal response and (ii) to separate the responses and anisotropy dynamics coming from the symmetric and asymmetric modes. Figure 7.3(a) shows the 2D-IR spectrum of a co-evaporated $MAPbI_3$ film at a delay of 1 ps. In this chapter, we use the convention of displaying the excitation frequency, ν_{ex}, along the horizontal axis and the probe frequency, ν_{pr}, along the vertical axis. As expected from the absorption spectra and the pump-probe measurements presented above, the signal associated with the bleaching of the 0$\rightarrow$1 transition of the symmetric bending mode is located at (ν_{ex};ν_{pr})=(1470; 1470) cm^{-1} and the ESA at (1470; 1445) cm^{-1}. As can be seen from the cross sections of the response for symmetric mode excitation at ν_{ex}=1470 cm^{-1} (Fig. 7.3(b)), at delay times longer than 10 ps, the signals associated with the excitation of the ν=1 state are substantially influenced and then overtaken by the thermal response. In addition to the symmetric bending responses, the 2D-IR spectra reveal cross peaks corresponding to the population of the symmetric mode ν_{pr}=1470 cm^{-1}, following excitation of asymmetric vibrations ν_{ex}=1560 cm^{-1}. Due

to the orthogonal orientation of the transition dipoles the response at the cross peaks is strongly depolarised. To extract the anisotropy decay originating from the symmetric mode reorientation, we focus on the responses in the center of the ESA feature at (1470;1445) cm^{-1}. Figure 7.3(c) presents the population dynamics measured with different pump and probe polarization and the blue dots Figure 7.3(d) show the extracted transient anisotropy decay for the co-evaporated $MAPbI_3$ film. After photoexcitation, the initial anisotropy is close to 0.4, which is the expected value for a random distribution of uncoupled dipoles.[235] The anisotropy decays on two clearly different timescales. The faster decay occurs on a timescale of <300 fs and decreases the anisotropy approximately by half. The longer 3 ps decay brings the anisotropy close to zero within the 6 ps observation window. We did not analyze the dynamics at longer times because at longer delays the signal becomes dominated by the thermal response. We also note that, as the anisotropy is analyzed in the center of the ESA peak, it reflects the reorientation for the majority of the molecules. However, some minor sub-ensemble of MA ions may have a shifted IR absorption line or/and faster spectral diffusion with a more pronounced orientational dynamics. Around 500 fs, the residual anisotropy still has a relatively high value of ∼0.2 for all samples. While the fast time-scale observed here agrees with the 400 fs timescale reported in previous NMR experiments,[217] the slow timescale of 3 ps has not been observed before. Longer (∼5 ps) timescales were predicted based on selective dynamics (artificially constrained frozen lead positions) MD simulations[202] and measured (5–14 ps) with quasi elastic neutron scattering on bulk material.[219,236] Independent of the preparation protocol and film morphology, all our thin-film samples demonstrate similar anisotropy dynamics (Figure 7.4(a)). We can hence exclude an influence of solvent residuals on the observed time scales, as two of the samples were fabricated with solvent free methods. We speculate that this explains part of the discrepancy between the reorientation times presented here and those recently derived from neutron scattering.[225]

7.2.2 MOLECULAR DYNAMICS SIMULATIONS

To obtain molecular-scale mechanistic insight into the origin and details of the organic cation dynamics, A. Walsh, J. M. Frost and T. L. C. Jansen undertook ab-initio molecular dynamic (MD) simulations starting in a pseudo-cubic geometry and at temperatures of 150, 300 and 450 K. To validate the simulations and to allow for a direct comparison to experimental results, the MD trajectories are used directly to calculate the absorption and the full 2D-IR response of the methylammonium NH_3^+ bending vibrations.[237,238] Figure 7.1(d) shows that the NH_3^+ bending absorption spectrum calculated with the procedure described above reproduces the experimental results well. The additional small peaks observed in the experimental data are probably associated with the CH_3 bending modes; the slightly different absorption cross section ratio for the symmetric and asymmetric modes is likely to originate from their assumption that the transition dipole direction of the local NH bending modes are perpendicular to the NH bonds. Figure 7.4(b) shows the calculated 2D-IR spectrum (perpendicular polarizations), which also reproduces the experimental results (Figure 7.3(a)). This proves the adequacy of the applied

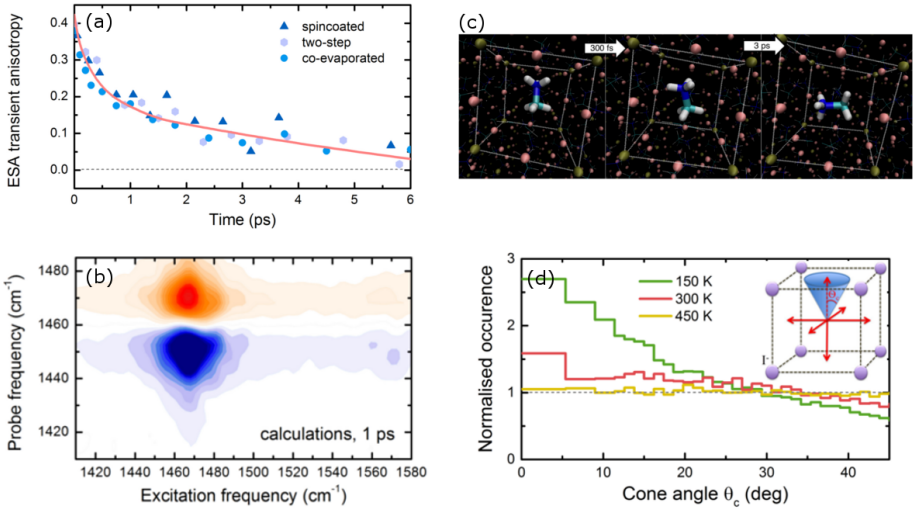

FIGURE 7.4. (a) Transient anisotropy in the peak of ESA response (ν_{ex} = 1470 cm^{-1}; ν_{pr} = 1445 cm^{-1}) for samples prepared using different techniques. The red line is a guide to the eye showing the transient anisotropy dynamics calculated based on MD simulations at 300 K. The time resolution was ∼100 fs for co-evaporated film and 300 fs for spincoated and two-step fabricated films. (b) The example of 2D-IR spectrum calculated with MD simulations. (c) An artist impression illustrating the motion of organic cation within the perovskite material. (d) Histogram of the simulated angular distribution of the MA dipoles at different temperatures normalized to the isotropic distribution. The inset illustrates the definition of the cone angle.

method for calculating the spectroscopic observables and, in turn, allows the further analysis of the anisotropy and orientation dynamics as taken explicitly from the MD simulations. The red line in Figure 7.3(d) shows the anisotropy decay in the (1470; 1445) cm^{-1} region of the calculated 2D-IR spectra, i.e. in the same area used to extract the experimental anisotropies. The simulated curve matches the experimental dynamics very well. Only the short-time component of the decay is slightly faster, which is likely to be the effect of experimental time resolution. First of all, this confirms the validity of the MD simulations and calculated orientation dynamics. Secondly, the theory-experiment match indicates the absence of intermolecular hopping of vibrational excitations. Intermolecular energy transfer is not included in the theoretical calculations and, in case it would play a role, the experimental anisotropy should decay faster as seen in other materials with fast vibrational excitation transfer.[65,234] Finally, the validated MD calculations can be used to identify the molecular picture behind the two observed timescales in anisotropy dynamics.
It is first verified that the anisotropy decay is due to rotation and not intramolecular vibrational population transfer. Simulating the 2D-IR spectra and extracting the anisotropy decay with fixed molecular orientations gives an anisotropy of 0.4 for all waiting times demonstrating that the origin of the observed decay is solely due to reorientation of the MA ions. This is not the case for the asymmetric peak at

1570 cm^{-1}, where two degenerate modes rapidly mix. The 2D-IR spectra at 150 K and 450 K were calculated and the extracted transient anisotropies are shown in Figure 7.3(d). It is apparent that at 150 K the anisotropy does not decay below 0.3, and that the anisotropy dynamics at 450 K are faster and lead to a nearly complete decay at 6 ps. Previous studies indicated a preferential orientation of the MD dipole parallel to the lattice axes[221] suggesting that at low temperatures the molecular dipole axis may be pinned to the lattice axes (Fig. 7.4(c), left). In Figure 7.4(d) histograms of the distribution of the angle between the molecular axis and the nearest of the lattice axis, which are equivalent in the simulated pseudo-cubic symmetry, are illustrated for the three simulated temperatures normalized to a random isotropic distribution of dipole directions. For 150 and 300 K there is a larger probability of finding an angle below 30 degree and lower probability of finding a larger angle. The 450 K data hardly deviate from the isotropic distribution. This suggests that the MA dipole preferentially points along one of the three lattice axes and is at 300 K confined within a semi-cone angle of about 30 degrees from each of these axes. We can consider a wobbling-in-a-cone/angular jump model,[239] where the rotational anisotropy is given by the equation:

$$r(t) = \frac{2}{5}\left(S^2 \exp\left\{ -\frac{t}{\tau_{jump}} \right\} + \left(1 - S^2\right) \exp\left\{ -\frac{1}{\tau_{jump}} + \frac{1}{\tau_{wob}} t \right\} \right) \qquad (7.1)$$

and where r(t) is the anisotropy, τ_{jump} is the effective jump time scale for 90 degree jumps, τ_{wob} is the time scale of the wobbling motion, and S is a constant depending on the semi-cone angle, Θ, of the wobbling motion given by the equation

$$S = \cos(\Theta)(1 + \cos(\Theta)/2 \qquad (7.2)$$

A biexponential fit to the simulated data results in a semi-cone angle of 31 degrees (S=0.625) from both the 150 K and 300 K data. The wobbling-in-a-cone timescale slows down from 130 fs to 1.1 ps, when cooling from 300 K to 150 K. We note that at 300 K the wobbling time fits well the 150 cm^{-1} vibration previously observed using Raman spectroscopy and assigned to librational motion,[240] which is the same as wobbling-in-a-cone motion. The time scale for the jump type motion is too long to fit for 150 K and 2.7 ps at 300 K. The 450 K data can be fitted with a single time scale of 570 fs and a small offset of 0.07 suggesting that the jump motion at this temperature is accelerated and no longer confined by the barriers. The small offset hints at the presence of an optimal orientation of the cation along one of the crystal axes, but may also be due to the error bars in the simulation data as at 450 K the cubic crystal structure prevails. It should be noted that all simulations were done for the pseudo-cubic phase and that experimentally at low temperature the structure is orthorhombic. This phase transition is thus not accounted for in the present simulations.

The combined experimental and theoretical results demonstrate that in the studied samples at 300 K the MA dipoles reorient on two distinct time scales. These are interpreted as a fast local wobbling-in-a-cone motion and slow 90 degrees jumps, respectively. We cannot fully exclude the presence of an additional slower decay

component, but the upper limit for the contribution of such a component is in the order of 0.07, corresponding to $< 20\%$ of all MA molecules moving on a slower time scale. These measurements thus dismisses the existence of large, slowly interconverting ferroelectric domains. However, we cannot rule out that the jump motion involves concerted motion of correlated MA domains.

7.3 CONCLUSION

To conclude, ultrafast 2D-IR vibrational anisotropy spectroscopy on the NH_3^+ symmetric bending vibration of MA and ab-initio MD were used to resolve in time the methylammonium cation rotation in different $MAPbI_3$ perovskites films. Excellent agreement was found between the experiment and the simulations. For all materials we observed similar dynamics with two characteristic timescales of molecular motion, which we identified as a fast wobbling-in-a-cone motion around the lattice axes and a relatively slow ($\sim$3 ps) jump-like reorientation of the molecular dipole (aligned with C–N-axis) between the different lattice axes. These timescales are directly relatable to the contribution to the dielectric response that comes from the molecular motion. Such a contribution is of extreme importance for the device physics of these materials, as the stability of excitons, polarons, and other quasi-particle states will depend on the response time of the dielectric constant. These findings represent the first real-time measurement of organic cation motion in organic-inorganic perovskite materials and provide access to the molecular mechanisms behind the optoelectronic properties of these materials.